
GENETIC HETEROGENEITY ANALYSIS USING GENETIC ALGORITHM AND NETWORK SCIENCE

Zhendong Sha
School of Computing
Queen's University
Kingston, Ontario, K7L 2N8
Canada
zhendong.sha@queensu.ca

Yuanzhu Chen
School of Computing
Queen's University
Kingston, Ontario, K7L 2N8
Canada
yuanzhu.chen@queensu.ca

Ting Hu
School of Computing
Queen's University
Kingston, Ontario, K7L 2N8
Canada
ting.hu@queensu.ca

August 15, 2023

ABSTRACT

Through genome-wide association studies (GWAS), disease susceptible genetic variables can be identified by comparing the genetic data of individuals with and without a specific disease. However, the discovery of these associations poses a significant challenge due to genetic heterogeneity and feature interactions. Genetic variables intertwined with these effects often exhibit lower effect-size, and thus can be difficult to be detected using machine learning feature selection methods. To address these challenges, this paper introduces a novel feature selection mechanism for GWAS, named **Feature Co-selection Network (FCS-Net)**. FCS-Net is designed to extract heterogeneous subsets of genetic variables from a network constructed from multiple independent feature selection runs based on a genetic algorithm (GA), a evolutionary learning algorithm. We employ a non-linear machine learning algorithm to detect feature interaction. We introduce the *Community Risk Score (CRS)*, a synthetic feature designed to quantify the collective disease association of each variable subset. Our experiment showcases the effectiveness of the utilized GA-based feature selection method in identifying feature interactions through synthetic data analysis. Furthermore, we apply our novel approach to a case-control colorectal cancer GWAS dataset. The resulting synthetic features are then used to explain the genetic heterogeneity in an additional case-only GWAS dataset.

Keywords Colorectal cancer · Epistasis · Genome-wide association studies · Heterogeneity analysis · Feature selection · Genetic algorithm · Network science

1 Introduction

The primary objective of case-control genome-wide association studies (GWAS) is the identification of disease-associated genetic variables [1]. Over the past two decades, GWAS has successfully linked thousands of genetic variables to disease susceptibility [2, 3, 4]. However, understanding the genetic underpinnings of disease and the identification of high-risk patients remains highly complex [5]. This complexity originates from multiple sources. First, genetic variables interact in a polygenic manner. Second, different genetic variables may interact with each other, a phenomenon known as epistasis [6]. Finally, similar to the hidden class problem in machine learning [7], disease-associated genetic variables may exhibit heterogeneity across different individuals [5]. The combined impact of these factors will diminish the effect size of disease-related variables, thus making their identification challenging.

The identification of heterogeneity is essential for the clinical translation of GWAS results. For instance, individuals who carry the BRA1/BRA2 gene, constituting about 1% of the population, exhibit a lifetime risk of developing breast cancer at 65%/45%, which is substantially higher than the population average of 12% [8].

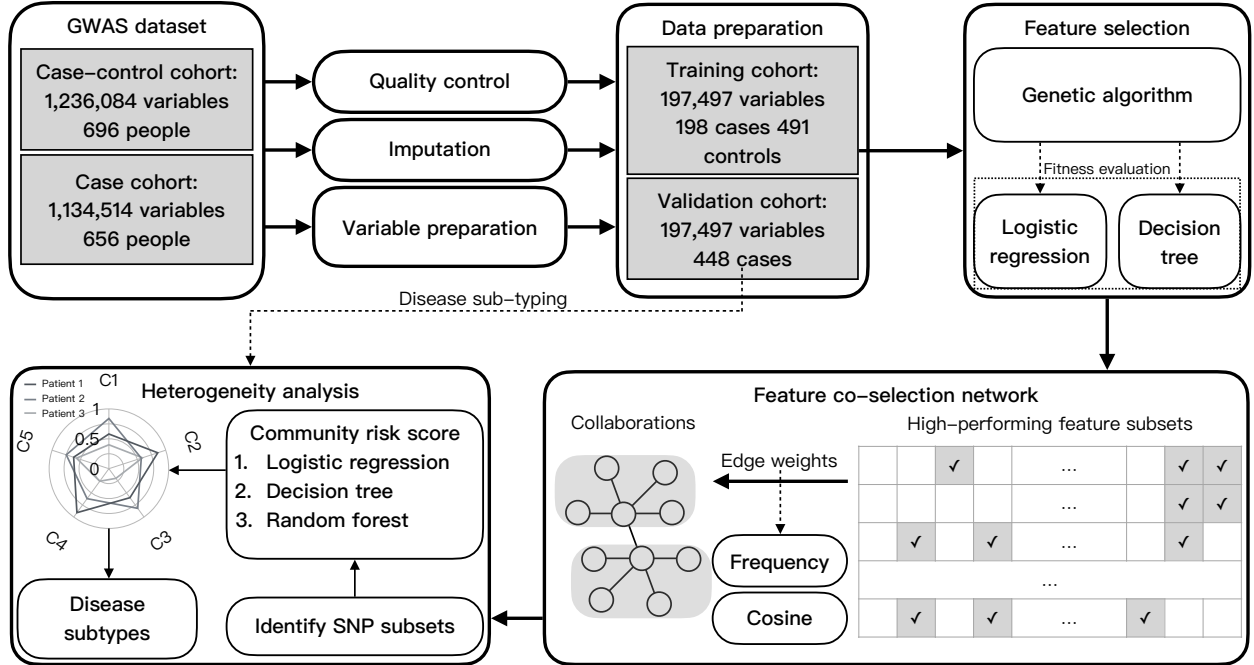


Figure 1: Overview of the FCS-Net framework. The GA-based feature selection algorithm is repeated multiple times to collect a set of high-performing feature subsets. A network of genetic variables is then constructed to capture co-selected feature collaborations. We apply a community detection algorithm to find frequently co-selected groups of features. These groups are used to create new synthetic features (community risk scores) to identify disease subtypes.

For this cohort, specialized prevention measures are recommended to improve treatment outcomes through early detection of disease onset [9].

Heterogeneity analysis is notably difficult in computational genetics due to the polygenic nature of genetic data and epistasis. The detection of risk associations can be challenging if patients of a particular subtype are underrepresented in the population [7]. A simulation study has shown that genetic heterogeneity can prevent the detection of genetic associations by multifactor dimensionality reduction (MDR), a software frequently employed to capture genetic interactions [10]. Therefore, prior to MDR analysis, it can be helpful to identify clusters of individuals with similar genetic backgrounds [10].

An effective heterogeneity analysis should address polygenicity and feature interaction together. This study introduces a novel approach, named **Feature Co-selection Network (FCS-Net)** (depicted in Figure 1), to characterize genetic heterogeneity. We frame the task of identifying heterogeneous feature subsets into a combinatorial optimization problem. We expect that multiple feature selection runs will yield diverse feature subsets when applied to a heterogeneous dataset. The feature selection algorithm is iterated multiple times to gather a set of high-performing feature subsets. A network of genetic variables is constructed to capture co-selected feature collaborations. A community detection algorithm is then leveraged to identify closely collaborated feature communities, which we interpret as evidence of heterogeneous disease associations within the dataset. Synthetic features reflecting the collective disease association of each variable community are created and hierarchical clustering algorithm is utilized to identify disease subtypes among diseased individuals based on these synthetic features. To confirm the capability of feature selection algorithms in identifying feature interactions, we undertake a simulation study based on GAMETES [11], a software package capable of generating intricate biallelic SNP disease models. We adopt the proposed framework on a case-control colorectal cancer GWAS dataset and carry out disease subtyping for another colorectal cancer GWAS dataset composed solely of diseased individuals.

2 Backgrounds

This section covers existing genetic heterogeneity analysis and feature selection methods. Feature selection plays a crucial role in identifying disease subtypes and mitigating the curse of dimensionality in high-dimensional datasets.

Clustering analysis has been employed to detect genetic heterogeneity in case-control studies [12]. Traditional clustering techniques such as k -Means [13], hierarchical clustering [14], and topological data analysis [15, 16, 17], have been leveraged to identify disease subtypes [5]. Nevertheless, these techniques do not scale well with high-dimensional data. The learning classifier system (LCS), in contrast, deviates from the standard single model approach by evolving a solution comprising multiple rules of clustering [18]. For instance, the extended Supervised Tracking and Classifying System (ExSTraCS) incorporates a feature-tracking strategy to identify features that have significant contributions to the accurate prediction of each instance [19, 20]. Clustering feature-tracking scores thus allows for the detection of underlying heterogeneous subtypes [7, 19]. The LCS Discovery and Visualization Environment (LCS-DIVE) [21] is an automated LCS model interpretation pipeline for biomedical data classification, LCS-DIVE utilizes feature-tracking scores and/or rules to characterize underlying heterogeneity through clustering.

For high-dimensional datasets, feature selection can mitigate the curse of dimensionality by discarding single nucleotide polymorphisms (SNPs) or genetic variables that are apparently not associated with the disease outcome. Existing literature groups feature selection methods into three categories: filter, wrapper, and embedded approaches [22, 23]. The filter approach typically operates independently of the classification algorithm. In contrast, the wrapper approach employs a classification model to evaluate the quality of a feature subset, potentially enhancing the predictive power of the selected feature subset [22, 24, 25]. However, the wrapper approach requires more computational resources, given its iterative evaluation of feature subsets, compared to the filter approach. The embedded approach concurrently performs feature selection and predictive model construction. Random forest [26] is a frequently used embedded feature selection algorithm [22, 24, 25]. Regularization techniques, such as Lasso or Ridge regression [27], can automatically select the most important features by integrating the loss function to penalize the inclusion of less important features. Current computational genetics research typically relies on filter approaches such as Relief-based methods [28, 29, 30, 31] and linkage disequilibrium (LD), i.e., the correlation structure among genetic variables [3, 32]. Relief-based methods utilize distance measures to estimate the importance of each feature but do not distinguish if the importance arises from uni-variable disease-association or interactions with other features [29].

One type of wrapper feature-selection approaches employ evolutionary algorithms to search for the most relevant and influential feature subset. Evolutionary algorithm is a population-based optimization strategy that simulates natural evolution. Evolutionary algorithms like genetic algorithm (GA)[33, 34, 35, 36, 37], particle swarm optimization (PSO)[38], and differential evolution (DE)[39] have been utilized to perform feature selection on biological microarray datasets. For GA, the evolution strategy for the population of solutions consists of two components. Crossover involves combining multiple solutions to create new solutions. Mutation introduces random changes to individual solutions to create new solutions. Specifically, GA searches for feature subsets by combining complementary subsets through crossover and making adjustments via mutation. A recent comparative study suggests that GA outperforms PSO on high-dimensional benchmark datasets from the UCI repository [40]. As a wrapper approach, GA-based feature selection relies on machine learning algorithms, such as linear regression [41], logistic regression [42], Naive Bayes [43, 44, 45], support vector machines (SVM)[36, 44, 46], and artificial neural networks (ANN)[47, 48, 49], to evaluate the quality of a feature subset.

3 Methodologies

Polygenic disease associations and epistasis are major obstacles in identifying genetic heterogeneity. Our study addresses these issues by considering the collaborations of features in subsets derived from multiple feature selection runs (Section 3.3). Additionally, this approach employs a feature construction method (Section 3.5) to capture the heterogeneous risk effects of different genetic variable subsets. The overview of our methodology is illustrated in Figure 1.

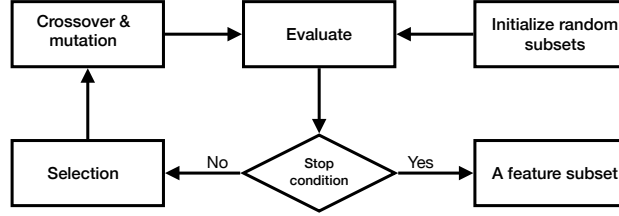


Figure 2: Flowchart of the GA algorithm

3.1 Colorectal cancer data

The GWAS datasets studied in this research are from colorectal cancer transdisciplinary (CORECT) consortium [50]. Genotyping is conducted using a custom Affymetrix genome-wide platform (the Axiom CORECT Set) on two physical genotyping chips (pegs) [50]. A total of 696 samples (200 colorectal cancer cases and 496 controls) are genotyped using the first chip, with each sample comprised of 1,236,084 SNPs. A total of 656 cases are genotyped using the second chip, with each sample comprised of 1,134,514 SNPs. The data processing procedure consists of three parts. The first part is the pre-imputation process, which is followed by the imputation of the missing values using the Michigan Imputation Server (MIS) [51]. The final step is the post-imputation process.

We perform quality control using PLINK [52], a whole-genome association analysis software tool. The pre-imputation process performs sample-level quality control to remove samples with a genotyping call rate less than 95%, sex labelling is not consistent with the chromosome, sample heterozygosity is not within three standard deviations from the mean. The pre-imputation process also perform SNP-level quality control to remove SNPs with minor allele frequency less than 1%. The two cohorts, genotyped using different chips, are merged and prepared to meet the requirements of MIS following the guidelines provided by its official tutorial¹.

During the imputation step, the Michigan Imputation Server is configured to use the eagle phasing algorithm [53], the hg19 reference panel and the mixed population option to accommodate the multi-racial population structure in Canada. The post-imputation process excludes low-quality SNPs based on the imputation R^2 of minimac3 ($R^2 > 0.3$) [51].

We extract all SNPs of the dataset used for MIS submission based on chromosome position and perform minor allele frequency and linkage disequilibrium filtering ($r^2 = 0.2$). A SNP is removed if its minor allele frequency is less than 0.01. IBD, or Identity by Descent, in PLINK is a computational method used to estimate the proportion of the genome where two individuals share alleles from a common ancestor. We remove first-degree relatives based on IBD. Samples in the second dataset are removed if the PI_HAT value is above 0.5 with any samples in the first dataset.

Finally, a total of 197,497 SNPs are selected for the subsequent analysis. The first dataset (training cohort) with both diseased cases ($N=198$) and healthy controls ($N=491$) is used for training, and the second dataset (validation cohort) is used for genetic heterogeneity analysis ($N=448$).

3.2 Genetic algorithm

We employ genetic algorithm (GA) as the foundational search strategy for feature selection (Figure 2). In this approach, GA represents a feature subset as an individual for population-based evolution, which is a binary vector with a length identical to the total number of features in the data. Here, a “1” suggests the selection of the corresponding feature, while a “0” indicates its exclusion. Each individual (selected feature subset) has a fitness value that indicates its overall relevance to the disease prediction. GA leverages tournament selection to select the best performing subsets from the population and utilizes uniform crossover with a probability of $cxpb$ and bit-flip mutation with a probability of $mutpb$ to evolve these individuals.

GA employs a machine learning algorithm to evaluate the fitness of its individual (feature subset). Fitness is assessed as the average testing area under the Receiver Operating Characteristic curve (AUC-ROC) from a five-fold cross-validation [54]. AUC-ROC is a key performance metric used to evaluate a predictive model’s ability to distinguish between classes. We use two machine learning algorithms provided by `scikit-`

¹<https://imputationserver.readthedocs.io/en/latest/prepare-your-data/>

learn[55] to evaluate the fitness of a feature subset. The first algorithm is logistic regression[56], due to its common adoption in polygenic risk prediction models. The second algorithm is the decision tree [57], which characterizes the interactions between features on the prediction. In Section 4.1, the difference between these two algorithms is investigated using synthetic data.

To address the high-dimensional nature of GWAS data, we implement two modifications to the GA algorithm. We introduce a size limit parameter, *size_limit*, which sets an upper limit on the number of features that can be selected in a feature subset. If mutation or crossover results in a selection exceeding the *size_limit*, we randomly deselect some features. This parameter aids in preventing overfitting by limiting the number of selected features. We have also noted that the crossover’s efficiency is undermined by the fact that decision trees only use a fraction of the features in the feature subset. Consequently, the decision tree-based GA only performs crossover on features included in the decision tree and deselects the unused ones. Parameter configurations for all experiments in this study are provided in Table 1.

The open-source package Distributed Evolutionary Algorithm in Python (DEAP) [58] is used to implement the GA. The population size is defined as *pop_size*, and the maximum number of generations is *ngen*. Tournament selection with *tour_size* is used to choose parents for crossover and mutation. Uniform crossover with a probability *cprob* and bit-flip mutation with a probability *mutpb* are utilized.

3.3 Feature collaboration identification

Given the stochastic nature of GA-based feature selection, each feature selection iteration yields different evolved feature subsets. Therefore, we conduct multiple GA runs and assume that the disease association of a feature pair (or their collaboration) can be reflected by their co-selection frequency across independent feature selection runs.

We assemble a set Γ of high-performing feature subsets derived from multiple GA-based feature selection iterations. A feature selection matrix M is constructed for Γ such that $M_{(i,j)} = 1$ if feature j is selected by subset i , and $M_{(i,j)} = 0$ otherwise. To quantify the degree of feature collaboration, we use the co-selection frequency and pairwise cosine similarity. The co-selection frequency counts the instances when a pair of features are co-selected, while the cosine similarity measures the selection similarity between features across different subsets.

We compute a feature co-selection frequency matrix A as follows:

$$A = M^T M, \quad (1)$$

where each element $A_{(i,j)}$ in A represents the number of evolved subsets in Γ that select both features i and j . One caveat of frequency-based identification is its inability to distinguish between collaborations involving frequently selected features and those that involve interdependent features crucial for predictive performance. To mitigate this limitation, we additionally employ cosine similarity to measure the likeness between pairs of features selected by different feature subsets.

The cosine similarity S_C of a feature pair (A, B) is computed as the cosine similarity between any two columns of the matrix M :

$$S_C(\vec{A}, \vec{B}) = \frac{\sum_{i=1}^n A_i B_i}{\sqrt{\sum_{i=1}^n A_i^2} \sqrt{\sum_{i=1}^n B_i^2}} \quad (2)$$

where A_i and B_i are the elements of column vectors \vec{A} and \vec{B} corresponding to subset i .

3.4 Feature co-selection network

The feature co-selection network, denoted as $G_{\text{coSel}} = (N, E)$ [42], is designed to capture strong collaborations between feature pairs within Γ . In this network, each node $n_i \in N$ represents a feature (genetic variable), and each edge $(n_i, n_j) \in E$ represents the collaboration between the corresponding variables.

To include the most important pair-wise feature collaborations, we impose edge weight thresholding. Specifically, we eliminate all edges in G_{coSel} with weights falling below τ_{occ} or τ_{cos} , where τ_{occ} and τ_{cos} denote the edge thresholds for co-selection frequency and cosine similarity, respectively.

To determine the values of τ_{occ} and τ_{cos} , we employ a network community detection algorithm (specifically, greedy [59]) on G_{coSel} and measure the quality of community separations using network modularity [59].

A network with high modularity will have dense intra-community node connections and sparse inter-community node connections. We optimize network modularity since we assume that collaborations between genetic variables exist in a modular form.

3.5 Community risk score

The Community Risk Score (CRS) aggregates the collective disease risk associated with a particular subset of genetic variables, equivalent to the network communities within the feature co-selection network. CRS can be used to estimate an individual’s disease risk.

To compute CRS, we randomly select 80% of the samples from the training cohort, which are then used to construct a predictive model for each variable subset corresponding to each CRS. This process will be repeated multiple times. After conducting multiple resampling runs, the CRS value for each individual is the averaged probabilistic outputs across multiple resampling runs.

In this study, we use the CRS value to estimate an individual’s disease risk with regard to a list of genetic variables. We use a variety of machine learning algorithms in parallel, including logistic regression, decision tree, and random forest, and perform 1000 resampling runs. The synthetic features generated by different communities are described using “C” followed by the community number. For example, the CRS value created for network community 1 is named C1.

3.6 Heterogeneity analysis using synthetic features

We perform clustering analysis to reveal disease heterogeneity within the validation cohort. Initially, we represent each observation using CRS values. This is followed by conducting hierarchical clustering using the Euclidean distance and the ward.D algorithm to group patients [60]. JASP [61], a platform-agnostic statistical software, facilitates the clustering analyses. The derived clusters are visualized using cluster means plots.

3.7 Functional enrichment analysis

We employ functional enrichment analysis to gain insight into a list of genetic variables, which is often used to translate disease-associated variables generated from genetic association analysis into biological insights. We use g:Profiler [62], a frequently updated software, to perform enrichment analysis. The software includes many popular biochemical pathway databases, such as Gene Ontology (GO), molecular function (GO:MF), biological process (GO:BP), cellular component (GO:CC), and common biological data sources such as Kyoto Encyclopedia of Genes and Genomes (KEGG), Reactome (REAC), WikiPathways (WP), Transfac (TF), Human Protein Atlas (HPA), CORUM protein complexes (CORUM), and Human Phenotype Ontology (HP). The statistical significance of functional enrichment terms is determined using the well-proven cumulative hypergeometric test. Terms surpassing a p -value threshold of 5% are considered as significant.

To explain the enrichment analysis derived from g:profiler, we use the procedure described in [63]. EnrichmentMap [64] and AutoAnnotate [65] are two popular enrichment analysis tools often used together. EnrichmentMap allows the visualization of enrichment results as a network of biological terms and comparison of enrichment results of different gene sets. In EnrichmentMap, nodes represent biological terms, and edges represent shared genes between two terms. AutoAnnotate identifies communities of connected terms and generates the theme of each community. Together, these tools help us to understand the functions of genes of interest.

4 Results

4.1 Simulation study

We conduct a simulation study to assess the efficacy of fitness evaluations in the GA based on logistic regression and decision tree algorithms to identify phenotype associated features and interactions. The simulation study is conducted using an open-access dataset from the PMLB [66], which is generated using the GAMETES tool [11]. GAMETES is frequently used in genetic studies to benchmark machine learning algorithms. The selected dataset² encompasses 1,000 attributes across two classes, with two attributes

²GAMETES_Epistasis_2_Way_1000atts_0.4H_EDM_1_EDM_1_1

Table 1: The parameter configurations for genetic algorithm.

Parameters	Simulation study		GWAS dataset	
	Logistic regression	Decision tree	Logistic regression	Decision tree
$ \Gamma $	1,000	1,000	10,000	10,000
<i>pop_size</i>	200	200	1,000	1,000
<i>size_limit</i>	5	5	200	200
<i>ngen</i>	50	50	50	100
<i>tour_size</i>	3	3	6*	6*
<i>cspb</i>	0.5	0.5	0.8*	0.8*
<i>mutpb</i>	0.2	0.2	0.2*	0.2*

$|\Gamma|$: Number of feature selection runs.

*: Determined through tuning three parameters, including $mutpb = \{0.2, 0.5, 0.8\}$, $cspb = \{0.2, 0.5, 0.8\}$, and $tour_size = \{3, 6, 9\}$.

exhibiting pure epistatic interaction. The objective of the feature selection process is to pinpoint these two interacting attributes.

For each fitness evaluation method (logistic regression or decision tree), the GA is run for 1,000 iterations. The effectiveness of fitness measures is evaluated by the frequency at which the two epistatic attributes are included in the best-performing feature subset evolved by the algorithm. A detailed description of the parameter configuration is provided in Table 1.

Our results show that when using the fitness evaluation based on the decision tree algorithm, the two epistatic features exhibit a co-occurrence frequency of 19 and a cosine similarity of 0.951. Conversely, using the logistic regression algorithm for fitness evaluation results in the GA’s failure to identify the feature pair, as one of the features is never selected. This finding underscores the considerable influence of the choice of fitness evaluation algorithm on the identification of interacting feature pairs. In subsequent sections, we perform heterogeneity analysis using both fitness measures to get a comprehensive understanding of the features (genetic variables) and their interactions in the CRC GWAS data (See Section 4.2 and Section 4.3).

4.2 Heterogeneity analysis based on decision tree

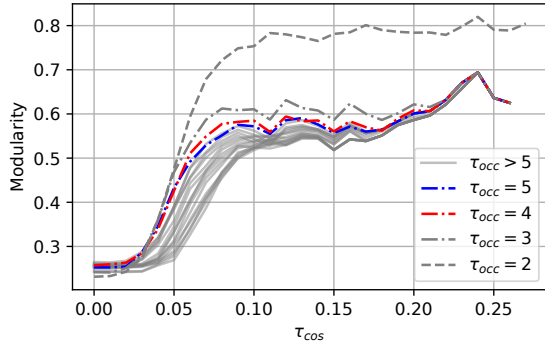
This section presents the results of the heterogeneity analysis employing the decision tree algorithm as the fitness measure. The parameter configuration for this analysis is provided in Table 1. Compared to logistic regression, the decision tree algorithm is capable of recognizing genetic interactions, which are considered to contribute more significantly to disease risk than individual variable effects [67]. To highlight frequently co-selected feature pairs, we utilize cosine similarity (defined in Section 3.4) in conjunction with the co-occurrence-based metric to filter edges for the feature co-selection network $G_{\text{coSel}}^{\text{DT}}$.

We begin by outlining the process of constructing the co-selection network $G_{\text{coSel}}^{\text{DT}}$ based on the decision tree algorithm. We then investigate the heterogeneous risk associations of each synthetic feature and identify distinct disease subtypes. Lastly, we undertake genetic enrichment analysis to pinpoint the biological terms associated with colorectal cancer.

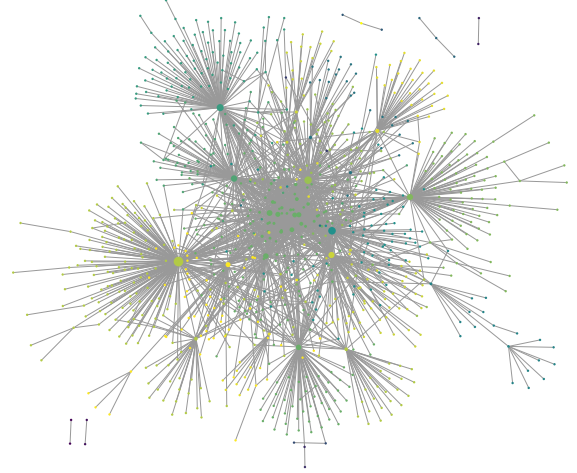
4.2.1 The construction of the feature co-selection network

The co-selection network $G_{\text{coSel}}^{\text{DT}}$ is created based on approximately 10,000 feature selection runs. The decision tree algorithm can identify feature interactions, and we leverage both cosine similarity and co-occurrence frequency to estimate the degree of interdependence between pairs of genetic variables (refer to Figure 3a). Cosine similarity is used to detect variable pairs with fewer co-occurrences but exhibit substantial correlations across the evolved feature subsets.

The choice of edge weight threshold values is a crucial factor determining the structure of the network. As the τ_{cos} threshold increases, the measured network modularity increases, indicating a growth in the structural modularity of these features generated by the decision tree based GA (see Figure 3a). Conversely, a high τ_{occ} threshold ($\tau_{\text{occ}} > 5$) leads to network fragmentation rather than modularization, generating an exceedingly high number of disconnected sub-networks (refer to Supplementary material Table S1). Hence, despite its favorable network modularity metric, a high τ_{occ} threshold is inappropriate for feature selection



(a) Determining the $G_{\text{coSel}}^{\text{DT}}$ network using feature co-selection number τ_{occ} and cosine similarity τ_{cos} .



(b) The $G_{\text{coSel}}^{\text{DT}}$ network generated using 10,000 feature selection runs based on decision tree with $\tau_{\text{occ}} = 5$ and $\tau_{\text{cos}} = 0.09$.

Figure 3: The determination and visualization of feature co-selection network based on decision tree. We determine the $G_{\text{coSel}}^{\text{DT}}$ network using feature co-selection number τ_{occ} and cosine similarity τ_{cos} . The $G_{\text{coSel}}^{\text{DT}}$ network is generated with $\tau_{\text{occ}} = 5$ and $\tau_{\text{cos}} = 0.09$. Network communities ($N=20$) are represented by colors. The size of node represents its degree.

analysis. The network modularity metric peaks when the τ_{cos} threshold exceeds 0.2, at which point the network consists of the most pertinent variable pairs with approximately 30 variables.

To balance network fragmentation and ensure the inclusion of sufficient genetic variables for our subsequent functional enrichment analysis, we establish the co-occurrence threshold τ_{occ} at 5 and the cosine similarity cut-off τ_{cos} at 0.09 (where the network modularity equals 0.582). If the τ_{cos} threshold is elevated to 0.13 (network modularity equals 0.591), only 300 genetic variables remain within the network. This loss of genetic variables, compared to choosing $\tau_{\text{cos}} = 0.09$ which contains 1036 variables, considerably constrains the effectiveness of the biological enrichment analysis.

4.2.2 Heterogeneous predictive performance of community risk scores

The constructed $G_{\text{coSel}}^{\text{DT}}$ network exhibits high network modularity. As depicted in Figure 3b, the network comprises 20 communities of genetic variables, 12 of which contain more than three genetic variables. In this section we investigate the heterogeneous predictive performance of synthetic features. Each synthetic feature corresponds to a distinct network community within the co-selection network.

A synthetic feature, named community risk score (CRS), estimates the risk impact of the genetic variables contained within each network community. For each community, we train logistic regression, decision tree, and random forest models using the training cohort of data. The probabilistic output generated by these predictive algorithms will be employed to represent individuals in the validation cohort, as explained in Section 3.5.

As demonstrated in Figure 4, the logistic regression algorithm (labelled as LR), is unable to recognize the disease risk of observations within the validation cohort. This may stem from the inability of the linear regression-based model to capture the feature interactions present within the feature communities. Further exploration of the predictive performance of CRSs based on decision tree and random forest algorithms (labelled as DT and RF), exhibits improved results across all communities. Lastly, although the CRSs based on the logistic regression algorithm exhibit weaker predictive performance than those based on the decision tree and random forest algorithms, the maximum risk impact across all 20 communities exhibits a better predictive power (refer to the sub-figure titled ‘‘Max’’ in Figure 4). This result suggests heterogeneity in the risk effects of the non-epistatic risk within the co-selection network $G_{\text{coSel}}^{\text{DT}}$.

4.2.3 Disease subtypes discovery

We identify disease subtypes using the hierarchical clustering algorithm (described in Section 3.6). The CRS values of the top 12 largest network communities in $G_{\text{coSel}}^{\text{DT}}$ are used to describe and represent diseased individuals in the validation cohort. We chose the decision tree algorithm over the logistic regression and random forest algorithms to generate CRS values. This ensures the consistency between the CRS generation and feature selection algorithms. The CRS values generated using different machine learning algorithms are similar to each other.

The community-specific predictive models are trained on the training cohort and used to predict the individuals in the validation cohort. We then use Euclidean distance and Ward.D linkage for heterogeneity analysis on the validation cohort. The results suggest that the diseased individuals in the validation cohort can be divided into four subtypes (see Figure 5). Subtype one does not have a CRS value with a median value higher than 0.5. The CRS with the highest risk is C9 (median=0.442), and the median of the rest of the CRSs is below 0.4. Subtype two also does not have a CRS value with a median value higher than 0.5. The CRS values with the highest risk are C3 (median=0.411) and C11 (median=0.409). The medians of C2 (median=0.421), C3 (median=0.411) and C5 (median=0.343) are higher than the other three subtypes. C12 (median=0.596) is at high risk in subtype three. Subtype four has a high risk in C6 (median=0.532) and C11 (median=0.534).

4.2.4 Functional enrichment analysis

We perform functional enrichment analysis on the 1036 genetic variables using g:Profiler [62] and EnrichmentMap [64] to identify the theme of the overall variables as well as each variable community. We submit a list of 1036 SNP rsIDs to g:Profiler and identify 210 biological terms with a p -value less than 0.05. The most significant term is *integral component of plasma membrane* (GO:0005887), and the theme of the most significant terms is *cell membrane*. We then visualize these terms using the EnrichmentMap tool for network visualization (Figure 6). We also perform enrichment analysis for genetic variables in each network community of $G_{\text{coSel}}^{\text{DT}}$ (distinguished by color). Communities 6 and 12 contain 6 and 9 terms that are not covered by the enrichment of the entire network.

The resulting network is annotated using the AutoAnnotate tool [65], which identifies groups of similar terms according to the network structure and determines the theme of each group by text-mining the names of biological terms. The largest term groups in the network are named *cell morphogenesis development* (containing 31 terms), *transmembrane transport ion* (containing 25 terms), *movement motility migration* (containing 13 terms), and *intracellular signal transduction* (containing 11 terms). There are also functional differences between different communities of $G_{\text{coSel}}^{\text{DT}}$. The genetic variables in Cluster 12 contain a theme covering six terms about paneth cell, while Cluster 4 linked to terms mainly distribute in *cell morphogenesis development*, *regulation assembly synapse*, and *periphery plasma membrane*. For more details about the enrichment analysis, please refer to Supplementary material Table S8.

4.3 Heterogeneity analysis based on logistic regression

This section provides a summary of the heterogeneity analysis based on feature selection runs using logistic regression as the fitness measure for the GA. The parameter configurations used for this analysis are described in Table 1. Unlike the decision tree algorithm, the logistic regression algorithm focuses on discovering genetic variables with high main effects. In this section, we examine the risk association of each synthetic feature or CRS value, and the disease heterogeneity that they reveal together. Additionally, we conduct a genetic enrichment analysis to identify the biological terms associated with colorectal cancer.

We created a feature co-selection network $G_{\text{coSel}}^{\text{LR}}$ by using a set of high-performing feature subsets Γ produced from approximately 10,000 GA runs. In this network, genetic variables are represented as nodes, and two types of weights, frequency of co-occurrences and cosine similarity, determine the edge between two nodes. The edge-cutoff values τ_{occ} and τ_{cos} are determined by optimizing the network modularity (see Figure 7b). The network with $\tau_{\text{occ}} = 7$ and $\tau_{\text{cos}} = 0.08$ yields the most suitable $G_{\text{coSel}}^{\text{LR}}$ network (modularity=0.253) for further analysis (visualized in Figure 7b). Some thresholds that could potentially yield better modularity are excluded as they resulted in an excessive number of network components or contained too many edges and nodes. We consider these networks not suitable for subsequent analysis. Detailed network investigation using different edge cut-offs is provided in the supplementary materials (Table S2). The resulting $G_{\text{coSel}}^{\text{LR}}$ network has 26 communities of genetic variables, with seven communities containing more than ten genetic

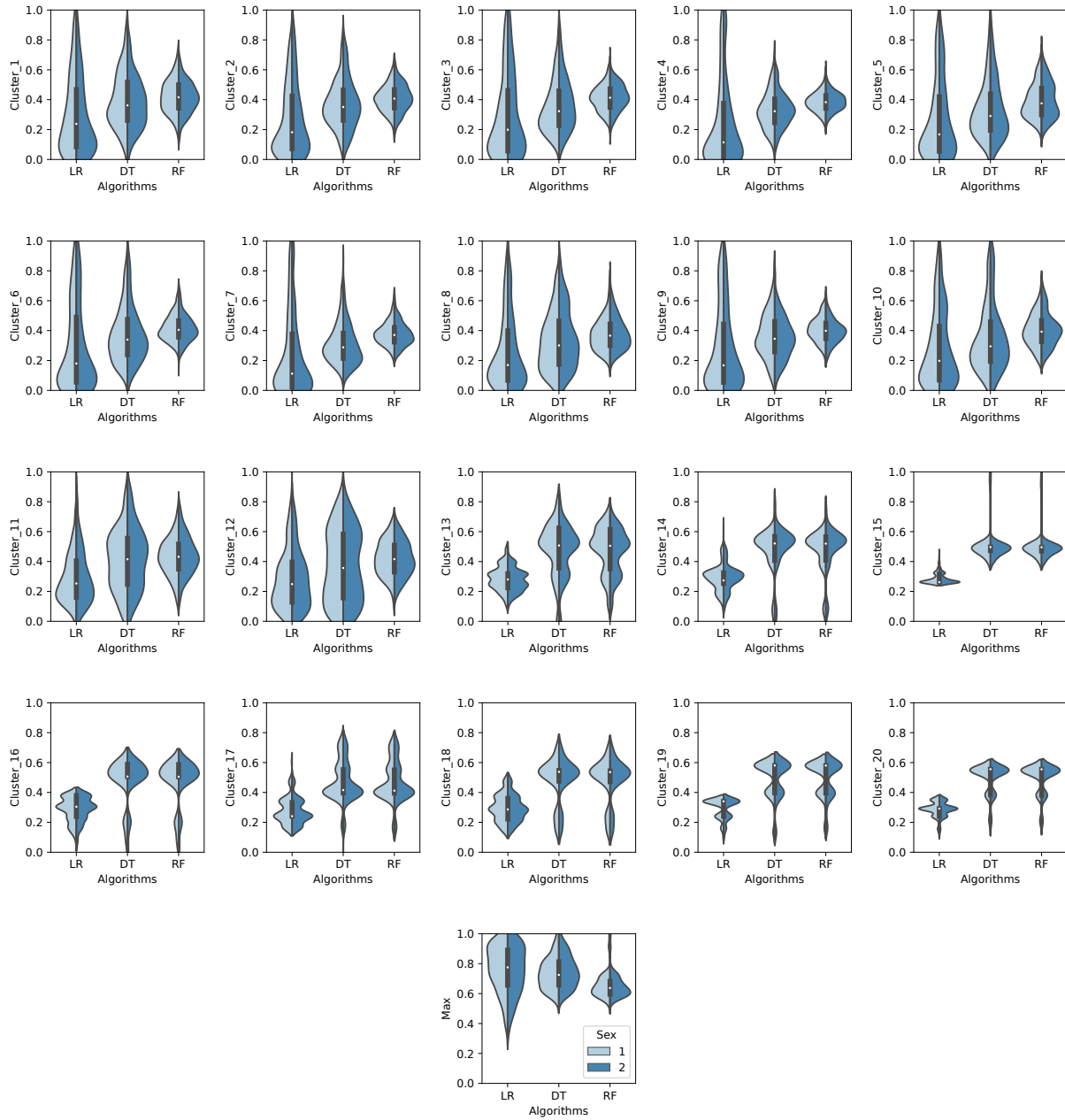


Figure 4: The heterogeneous risk predictive performance of the CRs based on decision tree. As many as 20 CRs are identified from $G_{\text{coSel}}^{\text{DT}}$ and used to describe individuals in the validation cohort. The maximum risk impact of all communities is summarized in sub-figure entitled “Max”.

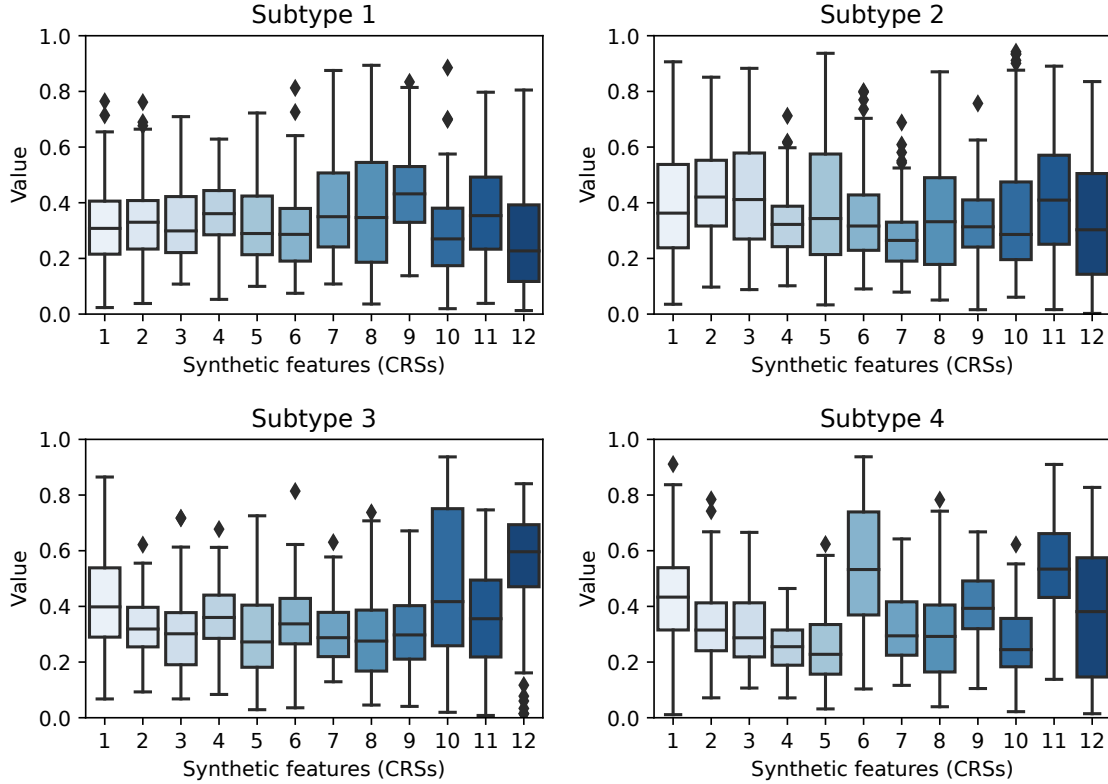


Figure 5: Cluster means plots for disease subtypes derived from CRSs based on decision tree.

variables. The network communities are visualized in Figure 7b using different colors and are used to create the synthetic features, as defined in Section 3.5.

We evaluate the predictive performance of each synthetic feature (CRS) using the resampling method described in Section 4.2.2. For each individual in the validation cohort, the CRS values are calculated as the mean across 1000 resampling runs. Figure 8 explains the heterogeneous risk-capturing capability of different CRS values, with each individual CRS only capturing the disease risk of a subset of individuals in the validation cohort. Notably, the decision tree-based algorithms (decision tree and random forest) generally outperform the linear regression algorithms in capturing disease risk. However, when we consider the maximum risk captured by all feature subsets, the linear regression algorithm performs the best.

We employ seven logistic regression-based CRSs, each consisting of more than ten genetic variables, to predict and represent the diseased individuals in the validation cohort for the analysis. Using hierarchical clustering algorithm based on Euclidean distance and Ward.D linkage, we identify four disease subtypes as shown in Figure 9. Among these subtypes, three contain at least one high-risk CRS with a median greater than 0.5. Subtype 1 does not have any CRS with a median higher than 0.5. The CRS with the highest risk is C1 (median=0.275), C4 (median=0.252) and C7 (median=0.259), and the median of the rest of the CRSs is below 0.2. Subtype 2 is at high risk in C2 (median=0.700). The remaining six CRSs present lower risk with a median of less than 0.2. Subtype 3 is at high risk in C3 (median=0.543) and C5 (median=0.561). The medians of all remaining five CRSs are below 0.2. Subtype 4 is at high risk in C6 (median=0.815). The remaining six CRSs present lower risk, except from C3 (median=0.214), all with a median less than 0.2.

We submitted a total of 820 genetic variables in $G_{\text{coSel}}^{\text{LR}}$ as well as seven community specific variable subsets for functional enrichment analysis using g:Profiler (see Supplementary materials Table S9 for details). As shown in Figure 10, the functional biological terms consist of two main groups. The theme of the largest group (N=78) is *cell signaling regulation* and the theme of the second largest group (N=44) is *transmembrane ion transport*.

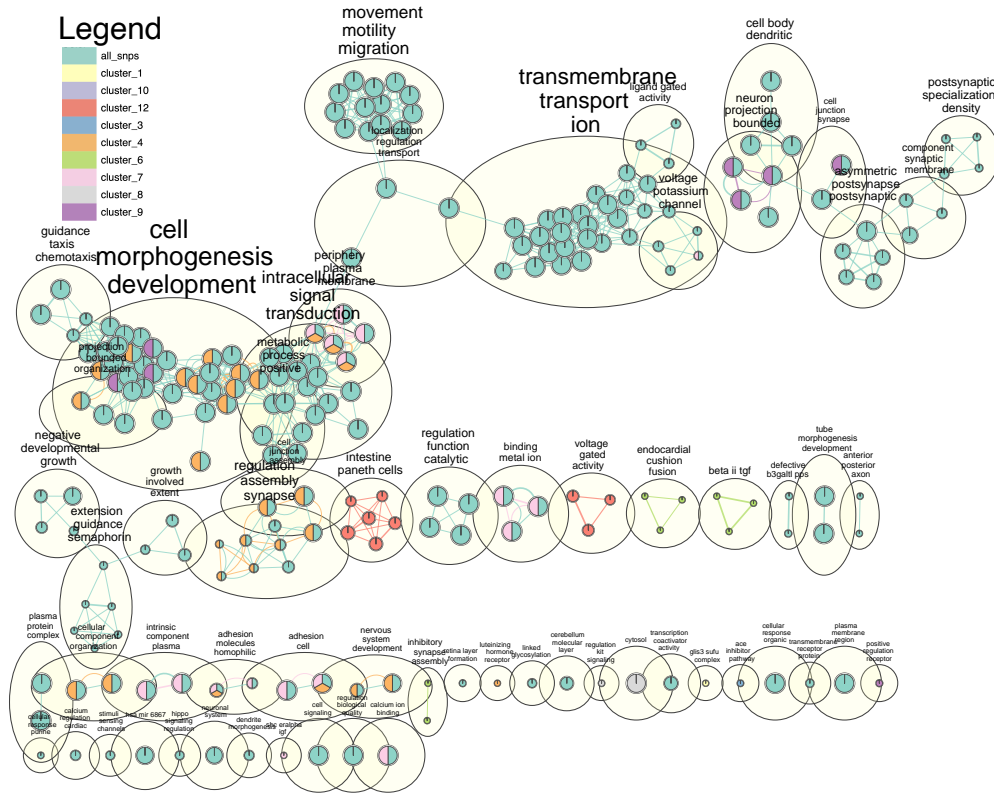


Figure 6: The functional enrichment analysis for $G_{\text{coSel}}^{\text{DT}}$ with $\tau_{\text{occ}} = 5$ and $\tau_{\text{cos}} = 0.09$. The functional terms (nodes) from different queries are represented by colors.

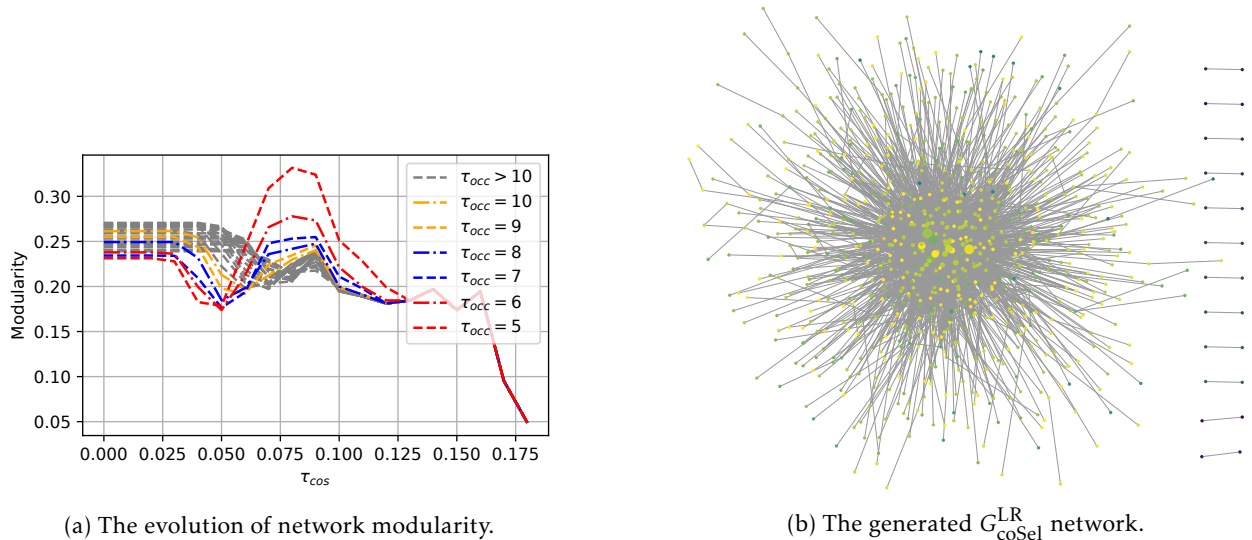


Figure 7: The determination and visualization of feature co-selection network based on logistic regression. We determine the $G_{\text{coSel}}^{\text{LR}}$ network with the highest network modularity based on edge cut-offs τ_{occ} and τ_{cos} . Network communities ($N=26$) of the resulting network are represented by colors and the size of node represents its degree.

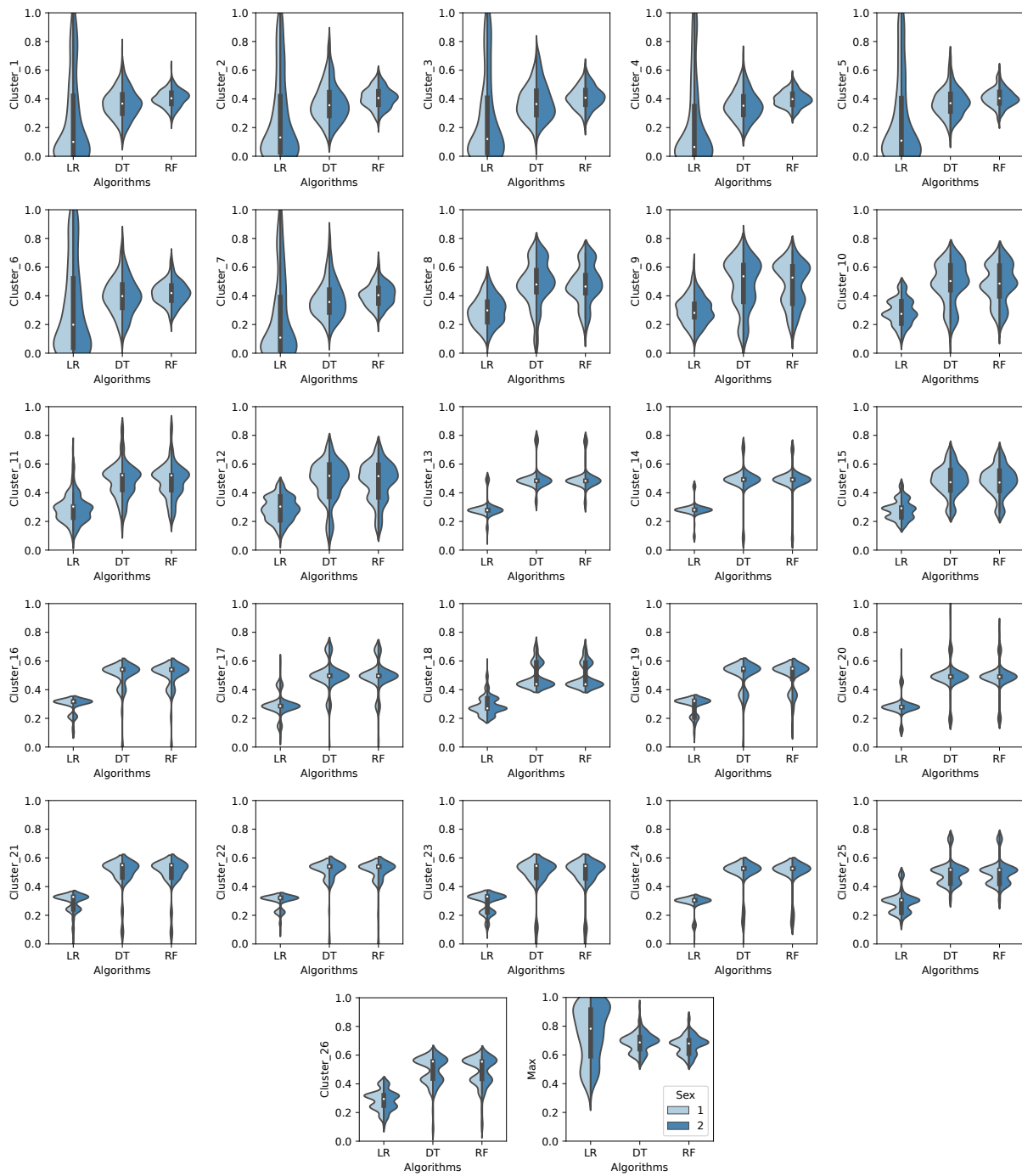


Figure 8: The heterogeneous risk predictive performance of the CRSs based on logistic regression. As many as 26 CRSs communities are identified from $G_{\text{coSel}}^{\text{LR}}$ on the validation cohort. The maximum risk impact of all communities is summarized in sub-figure entitled “Max”.

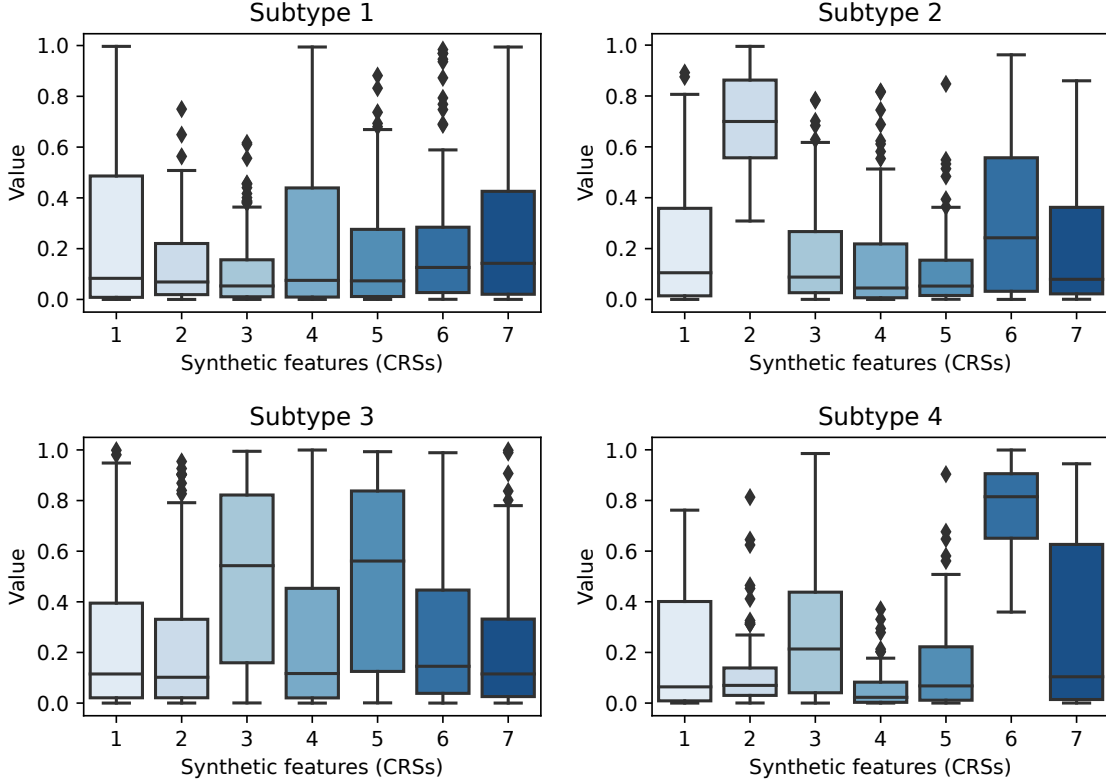


Figure 9: Cluster means plots for disease subtypes derived from CRSs based on logistic regression.

4.4 Over-fitting analysis

Since the number of observations in our dataset is relatively small compared to the number of features, we use all healthy controls in the training cohort for feature selection. This procedure may result in concerns regarding the over-fitting issue. Therefore, we develop new experiment to investigate the predictive performance of the proposed method for unseen observations.

We divide the entire dataset (including the training and validation cohorts) into training (80%) and testing (20%) splits. The training dataset is used as the input data for feature selection and to generate CRS values describing the observations in the test dataset. We then use the student t-test and AUC-ROC to investigate the ability of individual CRS values in discriminating between diseased and healthy individuals in the testing dataset.

We replicate the analysis for different fitness evaluation algorithms for the GA, namely the decision tree and logistic regression algorithms, and different network thresholds $(\tau_{occ}, \tau_{cos}) \in \{(3, 0.12), (4, 0.1), (4, 0.08)\}$ for decision tree-based GA and $(\tau_{occ}, \tau_{cos}) \in \{(3, 0.12), (38, 0.08), (55, 0.09)\}$ for logistic regression-based GA to determine the degree of overfitting.

The results indicate that for all parameter configurations, the CRS values containing more than 30 genetic variables will have significant ($p < 0.05$) discriminative capability on the testing dataset (see Figure S3, Figure S4, Figure S5, Figure S6, and Figure S7). Please refer to the Supplementary materials (Table S10 and Table S11) for detailed predictive performance quantified by AUC-ROC on the testing dataset. We conclude that both fitness algorithms have good resistance to overfitting.

5 Discussion

We propose a novel feature selection framework, named FCS-Net, for GWAS, based on the feature co-selection network, G_{coSel} . This network facilitates the depiction of collaborative interactions among genetic variables. It can be used to discern communities of genetic variables contributing to disease heterogeneity.

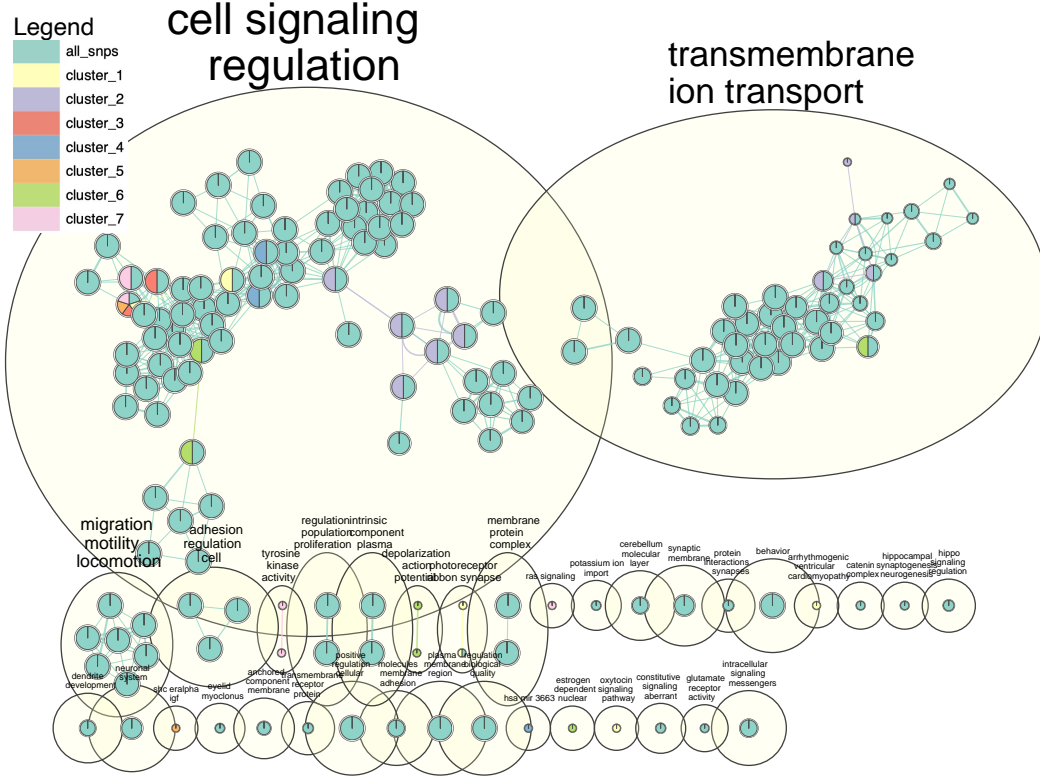


Figure 10: The functional enrichment analysis for $G_{\text{coSel}}^{\text{LR}}$ with $\tau_{\text{occ}} = 7$ and $\tau_{\text{cos}} = 0.08$. The functional terms (nodes) from different queries are represented by colors.

By offering a more intricate understanding of the relationships between genetic variables, FCS-Net provides a more detailed understanding than the traditional rank-based feature selection methods usually employed in GWAS.

5.1 The architecture of coSel network

The feature co-selection network, G_{coSel} , is formulated from a set of evolved high-performing genetic variable subsets. Within this network, nodes represent genetic variables, and the edges connecting pairs of variables are weighted by two distinct metrics: the frequency of co-occurrence between a pair of variables, and the cosine similarity. Clustering algorithms are employed to detect communities of genetic variables. The segmentation of variable subsets serves to create synthetic features or Community Risk Scores (CRSs), which are subsequently used to evaluate individual disease risk heterogeneity.

Our feature selection algorithm based on GA is guided to select feature subsets with varying characteristics using different fitness measures. Our results show that the co-selection network generated using the decision tree algorithm as fitness evaluation measure, $G_{\text{coSel}}^{\text{DT}}$ (Figure 3b), differs considerably from the network generated using the linear regression algorithm, $G_{\text{coSel}}^{\text{LR}}$ (Figure 7b).

The most significant difference between the $G_{\text{coSel}}^{\text{DT}}$ and $G_{\text{coSel}}^{\text{LR}}$ networks lies in their structural configurations. The $G_{\text{coSel}}^{\text{LR}}$ network features a central-peripheral architecture, while the $G_{\text{coSel}}^{\text{DT}}$ network exhibits a multi-centered architecture. This difference is attributed to the distinct mechanisms inherent to the two fitness measure algorithms. Linear regression-based logistic regression algorithms tend to select genetic variables with higher main effects. Conversely, the decision tree algorithm captures variables with feature interactions in addition to those with strong main effects. We consider that the multi-centered structure more accurately describes the structural modularity of the genetic architecture of Colorectal Cancer (CRC) than the central-peripheral architecture.

Another significant discrepancy between these two networks is on the edge weights. In this study, we employ two types of weights: the weight based on the frequency of co-occurrence, and the cosine similarity distance. For the $G_{\text{coSel}}^{\text{DT}}$ network, an elevated cosine similarity threshold considerably boosts the network’s modularity metric, from roughly 0.2 to 0.6. The $G_{\text{coSel}}^{\text{LR}}$ network, in contrast, lacks this property, exhibiting no modularity response to an increased cosine similarity threshold. The predictive mechanisms’ distinctness between logistic regression and decision tree algorithms contributes this difference. The decision tree algorithm can detect feature interactions, requiring features with such interactions to be selected simultaneously to improve the fitness value of a feature subset in the GA. Whereas, the logistic regression algorithm lacks such a mechanism, resulting in the evolved feature subsets produced by the GA not reflecting feature dependencies. The cosine distance used in our study plays a critical role in the construction of the G_{coSel} network. Unlike the commonly used threshold based on the number of co-occurrences [68], the cosine distance excludes edges that exist between frequently selected features, allowing the co-selection network’s edges to reflect the interplays between features.

We consider $G_{\text{coSel}}^{\text{DT}}$ more suitable for heterogeneity analysis than $G_{\text{coSel}}^{\text{LR}}$. This observation is based on our simulation study, which confirm that the decision tree algorithm enables the genetic algorithm in capturing feature interactions. Therefore, using the decision tree algorithm as the fitness measure of the GA can help uncover more disease-associated interaction genetic variables than the logistic regression algorithm does. Furthermore, the multi-centered network structure of $G_{\text{coSel}}^{\text{DT}}$ facilitates a more precise identification of heterogeneous subsets of genetic variables than the central-peripheral structure.

5.2 Heterogeneity analysis

In Section 4.1, we suggest that the decision tree-based fitness measure is preferred than logistic regression when dealing with high-dimensional datasets with feature interactions. Therefore, we replicate GA-based feature selection in this study, using both logistic regression and decision tree-based fitness measures. This approach allow us to utilize different machine learning techniques and discover features that influence disease risk through varying genetic mechanisms.

Our heterogeneity analysis successfully identifies disease subtypes in the validation cohort that exhibited heterogeneous risk across distinct CRS values, as represented in Figures 5 and 9. However, there is no correlation ($p = 0.622$) between subtypes generated based on different fitness evaluation algorithms. Moreover, no significant association is found between disease subtypes and gender.

5.3 Biological enrichment analysis

The biological enrichment analysis in this work utilizes the procedure documented in [63]. This protocol employs network science and natural language processing methods to extract themes related to CRC risk from a wide range of similar biological terms. In this section, we explore and compare the results of the biological enrichment analysis produced from the rsIDs in different coSel networks.

The $G_{\text{coSel}}^{\text{DT}}$ network contains 1036 genetic variables. The enrichment analysis of these 1036 rsIDs using g:profiler produces 210 significant ($p < 0.05$) terms. These biological terms have four major themes: *cell morphogenesis development* (N=31), *transmembrane ion transport* (N=25), *movement motility migration* (N=13), and *intracellular signal transduction* (N=11). To delve further into the role of these themes in CRC, we search for content in the NIH Library containing both the theme and CRC over the last five years. A total of 73 articles are found for *cell morphogenesis development*, 7 articles for *transmembrane ion transport*, 144 articles for *movement motility migration*, and 384 articles for *intracellular signal transduction*.

The $G_{\text{coSel}}^{\text{LR}}$ network contains 820 genetic variables. The enrichment analysis of these 820 rsIDs using g:profiler produces 171 significant ($p < 0.05$) terms. These biological terms have two major themes: *cell signaling regulation* (N=78) and *transmembrane ion transport* (N=44). We find a total of 5688 articles for cell signaling regulation and CRC and 7 articles for *transmembrane ion transport* and CRC over the last five years, using the NIH Library.

Comparing the enrichment analysis of genetic variables in different networks, we can identify the characteristics of the biological functions derived from different sets of rsIDs. We find that *transmembrane ion transport* is a common theme in both selection mechanisms. Generally, the $G_{\text{coSel}}^{\text{DT}}$ network generated based on the decision tree encompasses more complex biological functional terms, which may reflect the multi-centred network architecture of the G_{coSel} network. The biological functions found based on the linear regression

model have been more widely studied than those found based on the decision tree. An explanation might be that individual feature effects are still commonly used to select genetic variables for GWAS, and the genetic variables associated with feature interaction have not received enough attention in the literature yet.

6 Conclusions and future works

The existence of epistasis and heterogeneity can render the analysis and interpretation of high-dimensional genetic data challenging. This study transforms feature selection in GWAS into a combinatorial optimization problem, enabling heterogeneity analysis in the context of feature interaction. A crucial limitation of existing feature selection methods is that they only produce a list of features, overlooking the collaborative interplay among these features. To overcome this, FCS-Net leverages G_{coSel} to identify clusters of interacting variables associated with the disease. Simulation studies suggests that the use of the decision tree algorithm as the fitness evaluation for GA helps to recognize feature interactions, thereby enhancing the quality of heterogeneity analysis.

We propose several directions for future work. Firstly, our empirical findings provide new insights into feature selection methods based on the wrapper approach. We confirm that the search for variables with different disease-association mechanisms can be achieved by using various machine learning algorithms (e.g., logistic regression and decision tree) as the fitness measure of GA. As shown in Figures 3b and 7b, the network derived from the decision tree has a higher degree of modularity, which is undoubtedly beneficial for identifying heterogeneous variable subsets. Further research is needed to investigate the characteristics and capabilities of different machine learning algorithms to enhance the ability of GA or other wrapper feature selection approaches to capture disease-related variables.

Secondly, future studies could build upon the use of cosine similarity for identifying epistatic feature collaborations based on FCS-Net. Cosine similarity, as observed in our study, serves as an effective metric for epistasis discovery when decision tree-based fitness measures are applied. Our simulation study suggest a possible connection between such feature collaborations and feature interactions. This opens up opportunities for future research to explore second-order, and even higher-order, feature interactions. Our initial analysis on synthetic data encompassing third-order interactions indicates that decision tree-based GA can capture these interactions and represent them as a clique of three nodes on the feature co-selection network.

Lastly, addressing the limitations of hard community clustering algorithms is a crucial aspect for future research. Current greedy clustering algorithms segregate nodes into disjoint groups, operating under the assumption that a variable can only belong to a single group. However, in the field of cancer genomics, this assumption may not always hold true. The loss of essential variables can lead to a drop in the predictive performance of the corresponding CRS. Future work could employ network clustering algorithms that facilitate overlapping community detection [69, 70, 71] to overcome this constraint.

Data availability

The simulation datasets can be accessed through the Penn Machine Learning Benchmarks [66]. The GWAS data can be accessed through the colorectal cancer transdisciplinary (CORECT) consortium [50].

Supplementary materials

- Table S1: The evolution of the feature co-selection network based on decision tree by thresholds
- Table S2: The evolution of the feature co-selection network based on logistic regression by thresholds
- Figure S3: Overfitting analysis for feature co-selection network based on decision tree with $\tau_{\text{occ}} = 3$ and $\tau_{\text{cos}} = 0.12$
- Figure S4: Overfitting analysis for feature co-selection network based on decision tree with $\tau_{\text{occ}} = 4$ and $\tau_{\text{cos}} = 0.1$
- Figure S5: Overfitting analysis for feature co-selection network based on decision tree with $\tau_{\text{occ}} = 4$ and $\tau_{\text{cos}} = 0.08$
- Figure S6: Overfitting analysis for feature co-selection network based on logistic regression with $\tau_{\text{occ}} = 38$ and $\tau_{\text{cos}} = 0.08$

- Figure S7: Overfitting analysis for feature co-selection network based on logistic regression with $\tau_{\text{occ}} = 55$ and $\tau_{\text{cos}} = 0.09$
- Table S8: Biological enrichment analysis for the feature co-selection network based on decision tree
- Table S9: Biological enrichment analysis for the feature co-selection network based on logistic regression
- Table S10: The AUC-ROC of the CRSs derived from G_{coSel}^{DT}
- Table S11: The AUC-ROC of the CRSs derived from G_{coSel}^{LR}

Acknowledgements

We are grateful to Digital Research Alliance of Canada and Centre for Advanced Computing at Queen's University for providing high-performance computing infrastructures.

Conflict of Interest: No author has competing interests.

Funding information

This work was supported by the Natural Sciences and Engineering Research Council (NSERC) of Canada, Discovery Grant [RGPIN-2023-03302 to T.H.].

References

- [1] Jennifer E Rood and Aviv Regev. The legacy of the human genome project. *Science*, 373(6562):1442–1443, 2021.
- [2] Peter M Visscher, Loic Yengo, Nancy J Cox, and Naomi R Wray. Discovery and implications of polygenicity of common diseases. *Science*, 373(6562):1468–1473, 2021.
- [3] Peter M Visscher, Naomi R Wray, Qian Zhang, Pamela Sklar, Mark I McCarthy, Matthew A Brown, and Jian Yang. 10 years of GWAS discovery: Biology, function, and translation. *The American Journal of Human Genetics*, 101(1):5–22, 2017.
- [4] Ruth JF Loos. 15 years of genome-wide association studies and no signs of slowing down. *Nature Communications*, 11(1):1–3, 2020.
- [5] Andy Dahl and Noah Zaitlen. Genetic influences on disease subtypes. *Annual Review of Genomics and Human Genetics*, 21:413–435, 2020.
- [6] Naomi R Wray, Cisca Wijmenga, Patrick F Sullivan, Jian Yang, and Peter M Visscher. Common disease is more complex than implied by the core gene omnigenic model. *Cell*, 173(7):1573–1580, 2018.
- [7] Ryan John Urbanowicz, Angeline S Andrew, Margaret Rita Karagas, and Jason H Moore. Role of genetic heterogeneity and epistasis in bladder cancer susceptibility and outcome: a learning classifier system approach. *Journal of the American Medical Informatics Association*, 20(4):603–612, 2013.
- [8] Ali Torkamani, Nathan E Wineinger, and Eric J Topol. The personal and clinical utility of polygenic risk scores. *Nature Reviews Genetics*, 19(9):581–590, 2018.
- [9] Efrat Gabai-Kapara, Amnon Lahad, Bella Kaufman, Eitan Friedman, Shlomo Segev, Paul Renbaum, Rachel Beeri, Moran Gal, Julia Grinshpun-Cohen, Karen Djemal, Jessica B. Mandell, Ming K. Lee, Uziel Beller, Raphael Catane, Mary-Claire King, and Ephrat Levy-Lahad. Population-based screening for breast and ovarian cancer risk due to *brca1* and *brca2*. *Proceedings of the National Academy of Sciences*, 111(39):14205–14210, 2014.
- [10] Marylyn D Ritchie, Lance W Hahn, and Jason H Moore. Power of multifactor dimensionality reduction for detecting gene-gene interactions in the presence of genotyping error, missing data, phenocopy, and genetic heterogeneity. *Genetic Epidemiology*, 24(2):150–157, 2003.
- [11] Ryan J Urbanowicz, Jeff Kiralis, Nicholas A Sinnott-Armstrong, Tamra Heberling, Jonathan M Fisher, and Jason H Moore. Gametes: a fast, direct algorithm for generating pure, strict, epistatic models with random architectures. *BioData mining*, 5(1):1–14, 2012.

- [12] Nicholas J. Schork, Dani Fallin, Bonnie Thiel, Xiping Xu, Ulrich Broeckel, Howard J. Jacob, and Daniel Cohen. The future of genetic case-control studies. volume 42 of *Advances in Genetics*, pages 191–212. Academic Press, 2001.
- [13] Xiong Li, Liyue Liu, Juan Zhou, and Che Wang. Heterogeneity analysis and diagnosis of complex diseases based on deep learning method. *Scientific Reports*, 8(1):1–8, 2018.
- [14] Chikashi Terao, Boel Brynedal, Zuomei Chen, Xia Jiang, Helga Westerlind, Monika Hansson, Per-Johan Jakobsson, Karin Lundberg, Karl Skriver, Guy Serre, et al. Distinct hla associations with rheumatoid arthritis subsets defined by serological subphenotype. *The American Journal of Human Genetics*, 105(3):616–624, 2019.
- [15] Timothy SC Hinks, Tom Brown, Laurie CK Lau, Hitasha Rupani, Clair Barber, Scott Elliott, Jon A Ward, Junya Ono, Shoichiro Ohta, Kenji Izuhara, et al. Multidimensional endotyping in patients with severe asthma reveals inflammatory heterogeneity in matrix metalloproteinases and chitinase 3–like protein 1. *Journal of Allergy and Clinical Immunology*, 138(1):61–75, 2016.
- [16] Li Li, Wei-Yi Cheng, Benjamin S Glicksberg, Omri Gottesman, Ronald Tamler, Rong Chen, Erwin P Bottinger, and Joel T Dudley. Identification of type 2 diabetes subgroups through topological analysis of patient similarity. *Science Translational Medicine*, 7(311):311ra174–311ra174, 2015.
- [17] Monica Nicolau, Arnold J Levine, and Gunnar Carlsson. Topology based data analysis identifies a subgroup of breast cancers with a unique mutational profile and excellent survival. *Proceedings of the National Academy of Sciences*, 108(17):7265–7270, 2011.
- [18] Ryan J. Urbanowicz and Jason H. Moore. The application of pittsburgh-style learning classifier systems to address genetic heterogeneity and epistasis in association studies. In Robert Schaefer, Carlos Cotta, Joanna Kołodziej, and Günter Rudolph, editors, *Parallel Problem Solving from Nature, PPSN XI*, pages 404–413, Berlin, Heidelberg, 2010. Springer Berlin Heidelberg.
- [19] Ryan Urbanowicz, Ambrose Granizo-Mackenzie, and Jason Moore. Instance-linked attribute tracking and feedback for michigan-style supervised learning classifier systems. In *Proceedings of the 14th annual conference on Genetic and evolutionary computation*, pages 927–934, 2012.
- [20] Ryan J. Urbanowicz, Christopher Lo, John H. Holmes, and Jason H. Moore. Attribute tracking: Strategies towards improved detection and characterization of complex associations. In *Proceedings of the Genetic and Evolutionary Computation Conference, GECCO '18*, page 553–560, New York, NY, USA, 2018. Association for Computing Machinery.
- [21] Robert Zhang, Rachael Stolzenberg-Solomon, Shannon M Lynch, and Ryan J Urbanowicz. Lcs-dive: An automated rule-based machine learning visualization pipeline for characterizing complex associations in classification. *arXiv preprint arXiv:2104.12844*, 2021.
- [22] Manoranjan Dash and Huan Liu. Feature selection for classification. *Intelligent Data Analysis*, 1(1-4):131–156, 1997.
- [23] Isabelle Guyon and André Elisseeff. An introduction to variable and feature selection. *Journal of Machine Learning Research*, 3(Mar):1157–1182, 2003.
- [24] Huan Liu and Zheng Zhao. *Manipulating Data and Dimension Reduction Methods: Feature Selection*, pages 5348–5359. Springer New York, New York, NY, 2009.
- [25] Huan Liu, Hiroshi Motoda, Rudy Setiono, and Zheng Zhao. Feature selection: An ever evolving frontier in data mining. In *Proceedings of the Fourth International Workshop on Feature Selection in Data Mining*, pages 4–13. Proceedings of Machine Learning Research, 2010.
- [26] Leo Breiman. Random forests. *Machine learning*, 45(1):5–32, 2001.
- [27] Timothy Shin Heng Mak, Robert Milan Porsch, Shing Wan Choi, Xueya Zhou, and Pak Chung Sham. Polygenic scores via penalized regression on summary statistics. *Genetic Epidemiology*, 41(6):469–480, 2017.
- [28] Kenji Kira and Larry A Rendell. A practical approach to feature selection. In *Machine Learning Proceedings 1992*, pages 249–256. Elsevier, 1992.
- [29] Ryan J Urbanowicz, Melissa Meeker, William La Cava, Randal S Olson, and Jason H Moore. Relief-based feature selection: Introduction and review. *Journal of Biomedical Informatics*, 85:189–203, 2018.
- [30] Ryan J Urbanowicz, Randal S Olson, Peter Schmitt, Melissa Meeker, and Jason H Moore. Benchmarking relief-based feature selection methods for bioinformatics data mining. *Journal of Biomedical Informatics*, 85:168–188, 2018.

- [31] Cheng-San Yang, Li-Yeh Chuang, Yu-Jung Chen, and Cheng-Hong Yang. Feature selection using memetic algorithms. In *2008 Third International Conference on Convergence and Hybrid Information Technology*, volume 1, pages 416–423. IEEE, 2008.
- [32] Bjarni J Vilhjálmsson, Jian Yang, Hilary K Finucane, Alexander Gusev, Sara Lindström, Stephan Ripke, Giulio Genovese, Po-Ru Loh, Gaurav Bhatia, Ron Do, et al. Modeling linkage disequilibrium increases accuracy of polygenic risk scores. *The American Journal of Human Genetics*, 97(4):576–592, 2015.
- [33] W. Siedlecki and J. Sklansky. A note on genetic algorithms for large-scale feature selection. *Pattern Recognition Letters*, 10(5):335–347, 1989.
- [34] Murad Al-Rajab, Joan Lu, and Qiang Xu. Examining applying high performance genetic data feature selection and classification algorithms for colon cancer diagnosis. *Computer Methods and Programs in Biomedicine*, 146:11–24, 2017.
- [35] Mekaal Swerhun, Jasmine Foley, Brandon Massop, and Vijay Mago. A summary of the prevalence of genetic algorithms in bioinformatics from 2015 onwards. *arXiv preprint arXiv:2008.09017*, 2020.
- [36] Sabah Sayed, Mohammad Nassef, Amr Badr, and Ibrahim Farag. A nested genetic algorithm for feature selection in high-dimensional cancer microarray datasets. *Expert Systems with Applications*, 121:233–243, 2019.
- [37] Pilar García-Díaz, Isabel Sánchez-Berriel, Juan A Martínez-Rojas, and Ana M Diez-Pascual. Unsupervised feature selection algorithm for multiclass cancer classification of gene expression rna-seq data. *Genomics*, 112(2):1916–1925, 2020.
- [38] Cheng-Hong Yang, Huai-Shuo Yang, and Li-Yeh Chuang. Pbmldr: A particle swarm optimization-based multifactor dimensionality reduction for the detection of multilocus interactions. *Journal of Theoretical Biology*, 461:68–75, 2019.
- [39] Peng Wang, Bing Xue, Jing Liang, and Mengjie Zhang. Differential Evolution Based Feature Selection: A Niching-based Multi-objective Approach. *IEEE Transactions on Evolutionary Computation*, pages 1–1, 2022.
- [40] Nurhayati, Fajar Agustian, and Muhammad Dzil Ikram Lubis. Particle swarm optimization feature selection for breast cancer prediction. In *2020 8th International Conference on Cyber and IT Service Management (CITSM)*, pages 1–6, 2020.
- [41] Riccardo Leardi, R Boggia, and M Terrile. Genetic algorithms as a strategy for feature selection. *Journal of Chemometrics*, 6(5):267–281, 1992.
- [42] Zhendong Sha, Ting Hu, and Yuanzhu Chen. Feature selection for polygenic risk scores using genetic algorithm and network science. In *2021 IEEE Congress on Evolutionary Computation (CEC)*, pages 802–808, 2021.
- [43] Sérgio Francisco Da Silva, Marcela Xavier Ribeiro, João do ES Batista Neto, Caetano Traina-Jr, and Agma JM Traina. Improving the ranking quality of medical image retrieval using a genetic feature selection method. *Decision Support Systems*, 51(4):810–820, 2011.
- [44] Anne MP Canuto and Diego SC Nascimento. A genetic-based approach to features selection for ensembles using a hybrid and adaptive fitness function. In *The 2012 International Joint Conference on Neural Networks (IJCNN)*, pages 1–8. IEEE, 2012.
- [45] PEDRO SOUSA, PAULO CORTEZ, RUI VAZ, MIGUEL ROCHA, and MIGUEL RIO. Email spam detection: A symbiotic feature selection approach fostered by evolutionary computation. *International Journal of Information Technology & Decision Making*, 12(04):863–884, 2013.
- [46] Jae-Hyun Seo, Yong Hee Lee, and Yong-Hyuk Kim. Feature selection for very short-term heavy rainfall prediction using evolutionary computation. *Advances in Meteorology*, 2014, 2014.
- [47] Stephan M Winkler, Michael Affenzeller, Witold Jacak, and Herbert Stekel. Identification of cancer diagnosis estimation models using evolutionary algorithms: a case study for breast cancer, melanoma, and cancer in the respiratory system. In *Proceedings of the 13th Annual Conference Companion on Genetic and Evolutionary Computation*, pages 503–510, 2011.
- [48] Francisco Souza, Tiago Matias, and Rui Araújo. Co-evolutionary genetic multilayer perceptron for feature selection and model design. In *ETFA2011*, pages 1–7, 2011.
- [49] Stjepan Oreski and Goran Oreski. Genetic algorithm-based heuristic for feature selection in credit risk assessment. *Expert Systems with Applications*, 41(4):2052–2064, 2014.

- [50] Fredrick R Schumacher et al. Genome-wide association study of colorectal cancer identifies six new susceptibility loci. *Nature Communications*, 6:7138, Jul 2015.
- [51] Sayantan Das, Lukas Forer, Sebastian Schönherr, Carlo Sidore, Adam E Locke, Alan Kwong, Scott I Vrieze, Emily Y Chew, Shawn Levy, Matt McGue, et al. Next-generation genotype imputation service and methods. *Nature Genetics*, 48(10):1284–1287, 2016.
- [52] Shaun Purcell, Benjamin Neale, Kathe Todd-Brown, Lori Thomas, Manuel A.R. Ferreira, David Bender, Julian Maller, Pamela Sklar, Paul I.W. de Bakker, Mark J. Daly, and Pak C. Sham. Plink: A Tool Set for Whole-Genome Association and Population-Based Linkage Analyses. *The American Journal of Human Genetics*, 81(3):559–575, 2007.
- [53] Po-Ru Loh, Petr Danecek, Pier Francesco Palamara, Christian Fuchsberger, Yakir A Reshef, Hilary K Finucane, Sebastian Schoenherr, Lukas Forer, Shane McCarthy, Goncalo R Abecasis, et al. Reference-based phasing using the Haplotype Reference Consortium panel. *Nature genetics*, 48(11):1443–1448, 2016.
- [54] James A Hanley and Barbara J McNeil. The meaning and use of the area under a receiver operating characteristic (roc) curve. *Radiology*, 143(1):29–36, 1982.
- [55] F. Pedregosa, G. Varoquaux, A. Gramfort, V. Michel, B. Thirion, O. Grisel, M. Blondel, P. Prettenhofer, R. Weiss, V. Dubourg, J. Vanderplas, A. Passos, D. Cournapeau, M. Brucher, M. Perrot, and E. Duchesnay. Scikit-learn: Machine learning in Python. *Journal of Machine Learning Research*, 12:2825–2830, 2011.
- [56] David R Cox. The regression analysis of binary sequences. *Journal of the Royal Statistical Society: Series B (Methodological)*, 20(2):215–232, 1958.
- [57] Leo Breiman, Jerome H Friedman, Richard A Olshen, and Charles J Stone. *Classification and regression trees*. Routledge, 2017.
- [58] Félix-Antoine Fortin, François-Michel De Rainville, Marc-André Gardner, Marc Parizeau, and Christian Gagné. DEAP: Evolutionary algorithms made easy. *Journal of Machine Learning Research*, 13:2171–2175, jul 2012.
- [59] Aaron Clauset, Mark EJ Newman, and Cristopher Moore. Finding community structure in very large networks. *Physical Review E*, 70(6):066111, 2004.
- [60] Leonard Kaufman and Peter J Rousseeuw. *Finding Groups in Data: An Introduction to Cluster Analysis*, volume 344. John Wiley & Sons, 2009.
- [61] JASP Team. JASP (Version 0.10.2)[Computer software], 2019.
- [62] Uku Raudvere, Liis Kolberg, Ivan Kuzmin, Tambet Arak, Priit Adler, Hedi Peterson, and Jaak Vilo. g:Profiler: a web server for functional enrichment analysis and conversions of gene lists (2019 update). *Nucleic Acids Research*, 47(W1):W191–W198, 05 2019.
- [63] Jüri Reimand, Ruth Isserlin, Veronique Voisin, Mike Kucera, Christian Tannus-Lopes, Asha Rostami-anfar, Lina Wadi, Mona Meyer, Jeff Wong, Changjiang Xu, et al. Pathway enrichment analysis and visualization of omics data using g: Profiler, GSEA, Cytoscape and EnrichmentMap. *Nature Protocols*, 14(2):482–517, 2019.
- [64] Daniele Merico, Ruth Isserlin, Oliver Stueker, Andrew Emili, and Gary D. Bader. Enrichment map: A network-based method for gene-set enrichment visualization and interpretation. *PLOS ONE*, 5(11):1–12, 11 2010.
- [65] M Kucera, R Isserlin, A Arkhangorodsky, and GD Bader. Autoannotate: A cytoscape app for summarizing networks with semantic annotations [version 1; peer review: 2 approved]. *F1000Research*, 5(1717), 2016.
- [66] Joseph D Romano, Trang T Le, William La Cava, John T Gregg, Daniel J Goldberg, Praneel Chakraborty, Natasha L Ray, Daniel Himmelstein, Weixuan Fu, and Jason H Moore. PMLB v1.0: an open-source dataset collection for benchmarking machine learning methods. *Bioinformatics*, 38(3):878–880, 10 2021.
- [67] Evan A. Boyle, Yang I. Li, and Jonathan K. Pritchard. An expanded view of complex traits: From polygenic to omnigenic. *Cell*, 169(7):1177–1186, 2017.
- [68] Alessandro Miani, Thomas Hills, and Adrian Bangerter. Interconnectedness and (in)coherence as a signature of conspiracy worldviews. *Science Advances*, 8(43):eabq3668, 2022.
- [69] Chiheb-Eddine Ben N’Cir, Guillaume Cleuziou, and Nadia Essoussi. Overview of overlapping partitioned clustering methods. In *Partitional Clustering Algorithms*, pages 245–275. Springer, 2015.

- [70] David M Blei, Andrew Y Ng, and Michael I Jordan. Latent dirichlet allocation. *Journal of Machine Learning Research*, 3:993–1022, 2003.
- [71] Jaewon Yang and Jure Leskovec. Overlapping community detection at scale: A nonnegative matrix factorization approach. In *Proceedings of the Sixth ACM International Conference on Web Search and Data Mining*, WSDM '13, page 587–596, New York, NY, USA, 2013. Association for Computing Machinery.